

# Simultaneous calibration of optical tweezers spring constant and position detector response

Antoine Le Gall,<sup>1</sup> Karen Perronet,<sup>1</sup> David Dulin,<sup>1</sup> André Villing,<sup>1</sup>  
Philippe Bouyer,<sup>1</sup> Koen Visscher,<sup>1,2</sup> and Nathalie Westbrook<sup>1,\*</sup>

<sup>1</sup>Laboratoire Charles Fabry de l'Institut d'Optique, CNRS et Université Paris Sud 11,  
Campus Polytechnique, 2 avenue Fresnel, 91127 Palaiseau cedex, France

<sup>2</sup>Departments of Physics, Molecular and Cellular Biology, and College of Optical Sciences,  
University of Arizona, Tucson, Arizona 85721, USA

\*[nathalie.westbrook@institutoptique.fr](mailto:nathalie.westbrook@institutoptique.fr)

**Abstract:** We demonstrate a fast and direct calibration method for systems using a single laser for optical tweezers and particle position detection. The method takes direct advantage of back-focal-plane interferometry measuring not an absolute but a differential position, i.e. the position of the trapped particle relative to the center of the optical tweezers. Therefore, a fast step-wise motion of the optical tweezers yields the impulse response of the trapped particle. Calibration parameters such as the detector's spatial and temporal response and the spring constant of the optical tweezers then follow readily from fitting the measured impulse response.

© 2010 Optical Society of America

**OCIS codes:** (350.4855) Optical tweezers; (170.4520) Optical confinement and manipulation; (120.4640) Optical instruments; (120.1880) Detection; (180.0180) Microscopy.

---

## References and links

1. K. Visscher, S. P. Gross and S. M. Block, "Construction of multiple-beam optical traps with nanometer-resolution position sensing," *IEEE J. Quantum Electron.* **2**, 1066–1076 (1996).
2. F. Gittes and C. Schmidt "Interference model for back-focal-plane displacement detection in optical tweezers," *Opt. Lett.* **23**, 7–9 (1998).
3. K. C. Neuman, and A. Nagy, "Single-molecule force spectroscopy: optical tweezers, magnetic tweezers and atomic force microscopy," *Nat. Methods* **5**, 491–505 (2008).
4. K. Visscher, M. J. Schnitzer, and S. M. Block, "Single kinesin molecules studied with a molecular force clamp," *Nature* **400**, 184–189 (1999).
5. Y. R. Chemla, "Revealing the base pair stepping dynamics of nucleic acid motor proteins with optical traps," *Phys. Chem. Chem. Phys.* **12**, 3080–3095 (2010).
6. S. F. Tolić-Nørrelykke, E. Schäffer, J. Howard, F. S. Pavone, F. Jülicher, and H. Flyvbjerg, "Calibration of optical tweezers with positional detection in the back focal plane" *Rev. Sci. Instrum.* **77**, 103101–11 (2006).
7. M. W. Allersma, F. Gittes, M. J. deCastro, R. J. Stewart, and C. F. Schmidt, "Two-Dimensional Tracking of ncd Motility by Back Focal Plane Interferometry," *Biophys. J.* **74**, 1074–1085 (1998).
8. K. Vermeulen, J. van Mameren, G. Stienen, E. Peterman, G. Wuite, and C. Schmidt, "Calibrating bead displacements in optical tweezers using acousto-optic deflectors," *Rev. Sci. Instrum.* **77**, 013704 (2006).
9. K. Berg-Sørensen, L. B. Oddershede, E. L. Florin, and H. Flyvbjerg, "Unintended filtering in a typical photodiode detection system for optical tweezers," *J. Appl. Phys.* **93**, 3167–3176 (2003).
10. K. Berg-Sørensen, and H. Flyvbjerg, "Power spectrum analysis for optical tweezers," *Rev. Sci. Instrum.* **75**, 594–612 (2004).
11. P. M. Hansen, I. Tolić-Nørrelykke, H. Flyvbjerg, and K. Berg-Sørensen, "tweezercalib 2.1: Faster version of MATLAB package for precise calibration of optical tweezers," *Comput. Phys. Commun.* **175**, 572–573 (2006).

## 1. Introduction

Optical tweezers are ideally suited for manipulation of micron and submicron-sized particles. The subsequent application of high-resolution position detection methods, e.g. back focal plane detection [1, 2], and accurate calibration of the tweezers' spring constant then readily enabled the measurement of displacements and forces by individual biomolecular motors [3–5].

When the same laser beam is used for optical trapping and position detection, the exclusive experimental set-up discussed here, back-focal plane (BFP) detection reports on the displacement of the trapped particle with respect to the center of the optical tweezers. Forces are readily computed by multiplication of displacement and the calibrated spring constant of the tweezers. Over the years a variety of calibration methods have been proposed, although only a few simultaneously yield the calibration parameters for the position sensor and the spring constant [6,7]. Position detector calibration used to be laborious when surface mounted beads were used and scanned through the laser beam to determine the average detector response. For example, there may be considerable variability in the axial position of the particle with respect to the tweezers center which affects the lateral calibration coefficients and which can only be minimized by sufficient averaging. This situation was remedied by Vermeulen et al. [8] who acquired the detector response by very rapidly scanning the trapping laser beam over the particle (so fast as not to allow any appreciable particle motion). This method enables online calibration of each trapped particle used in an experiment, but does not simultaneously yield the tweezers spring constant. Furthermore, it requires rapid scanning of the optical tweezers, something not always possible with all set-ups, even when utilizing acousto-optical deflectors (AOD) for positioning of the optical tweezers. A power spectrum density (PSD) analysis of the particle position in the optical tweezers circumvents such practical limitations and is capable of providing the optical tweezers spring constant as well as the linear detector response [7].

Here we present an alternative method which measures the impulse response of the BFP detector yielding both the detector response as well as the optical tweezers spring constant, and which may lend itself better for quick online use during day-to-day experiments. Our impulse response method can also account for the temporal response of the specific quadrant photodiode (QPD) [9] used as part of the BFP set-up and for the limited response time of the device (piezo mirror, AOD) moving the optical tweezers laser beam. Using an AOD positioned in the optically conjugated plane of the back focal plane of the microscope objective, the trap is moved in a step-wise fashion from one position to another. The displacement of the optical tweezers is then only limited by the temporal response of the AOD given by  $T_r = 0.64D/V$ , where  $T_r$  is the time interval for the light intensity to go from 10% to 90% of maximum value in response to an acoustic step,  $D$  is the laser  $1/e^2$  waist and  $V$  the acoustic velocity. In our conditions this response time is  $1.6 \mu\text{s}$ , much shorter than any of the other typical temporal responses in the system (QPD, particle in the trap). As the trap is rapidly moved, the bead cannot follow the trap motion instantaneously, but rather relaxes towards the new trap position with a relaxation time given by the ratio of the viscous drag coefficient and the tweezers spring constant. Since the BFP position detector as implemented here reports on the position of the particle with respect to the center of the optical tweezers, a sudden trap displacement yields the impulse response rather than the step response of the particle, visible as a spike in the QPD signal. If the QPD were of infinite temporal bandwidth the height of the peak would equal the trap displacement, while the relaxation curve yields the tweezers spring constant. However, since we used a QPD with limited temporal response at a wavelength of 1064 nm [9], the measured response proved a convolution of the impulse response of the particle in the optical trap and that of the photodiode. Upon fitting the measured response we found excellent agreement with power spectral analysis as well as with the equi-partition methods.

## 2. Materials and methods

Experiments were done using an Olympus IX70 inverted microscope and an oil immersion objective (Olympus PlanApo 60X, NA=1.45). A Nd:YAG laser (Quantum Laser, model Forte 1064, TEM<sub>00</sub>) delivering up to 1W of power was used for trapping. The laser beam is diffracted by an AOD (Intra Action Corp. DTD-274HA6 with one AOD removed) allowing the steering of the trap along one axis. To steer the trap horizontally in the sample the AOD needs to be conjugated with the back focal plane of the objective. To do so the AOD is located at the focal plane of the first lens, L1, of the beam expander used to fill the pupil of the objective. The first-order diffracted beam by the AOD was sent into two additional 1:1 telescopes used for axial steering of the trap and for combining the optical tweezers with the excitation optical path used for Total Internal Reflection Fluorescence (TIRF) microscopy (Fig. 1).

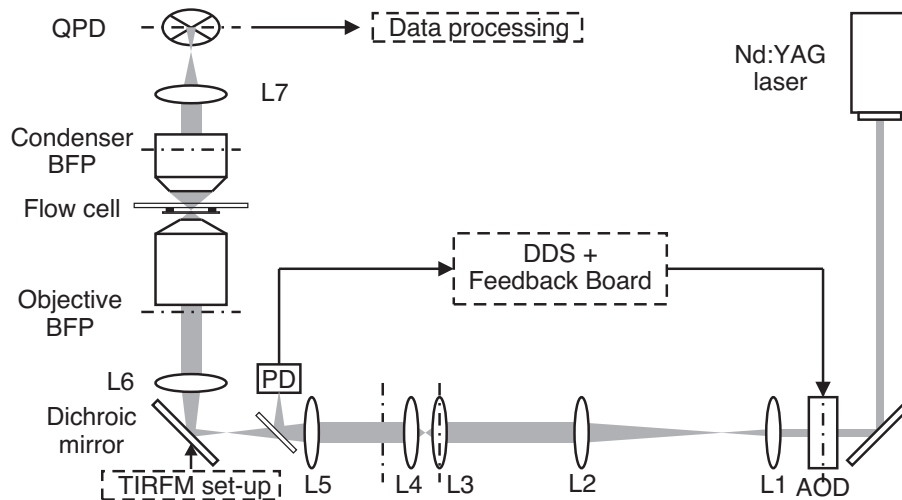


Fig. 1. Experimental set-up. Dashed lines represent the conjugated planes at the center of the AOD and on the QPD. A cover glass and a photodiode (PD) were used to probe the laser power before the objective in order to keep it constant via the feedback board. Focal lengths are (in mm) 175, 500, 50, 50, 300, 300 and 40 for L1 to 7.

The first-order diffracted beam was coupled into the oil immersion objective via a dichroic mirror (Chroma, z488/1064rpc), and transmitted light was collected with a high numerical aperture condenser (Olympus Aplanat Achromat, NA=1.4) and directed to the QPD (SPOT-9DMI, OSI Optoelectronics). An additional lens, L7, was positioned between the condenser and the QPD to make the appropriate conjugation of the QPD with the BFP of the microscope objective and the AOD. All 4 signals from the QPD quadrants were digitized simultaneously at a rate of 65536 Hz using a Delta Sigma DAC (National Instrument, PCI 4474) and further processed using LabView 8.2. We note that, before calibration, displacement signals as computed from the sampled quadrant values are dimensionless since these are normalized by the sum of all quadrants values. A home-built Direct Digital Synthesizer (DDS) was used to generate the radio frequency signal driving the AOD and controlling the trap displacement in the sample. The DDS was addressed via computer using a dedicated processor generating highly reproducible command sequences. A fraction of the laser beam power was picked off using a microscope cover glass and directed towards a photodiode to complete a feedback loop controlling the AOD driving signal amplitude as to maintain constant laser power at the entrance of the objective. For the baseline position detector signal to be constant for different AOD frequencies we

found it crucial that the AOD was accurately located at the proper conjugate plane - a requirement that is more easily satisfied when L1 has a not too short focal length - and that constant power is maintained even though the position signals were normalized by the QPD sum signal. The AOD was calibrated by sending a 10 kHz step-ramp to the AOD over a range of 400 kHz around a center frequency of 26.2 MHz. For every step, 25 images of a trapped bead were acquired with a CCD camera (uEye, UI-2250-M), averaged, and processed with ImageJ using the “particle tracker and detector” plug-in to localize the position of the bead in pixels in the sample. Pixels dimensions corresponded to 22.27 nm by 22.27 nm in the sample plane as calibrated using a 10  $\mu\text{m}$ -division stage micrometer. The AOD response was found to be linear within the frequency range used, yielding an effective trap displacement of 1.54 nm/kHz. Silica beads were purchased from Bangs Laboratories (SS03N, 1  $\mu\text{m}$  diameter) and diluted to 1:10<sup>5</sup> (v/v) in de-ionized water from an initial concentration of 10% wt stock beads. The solution was injected into a 5 mm wide chamber made of two narrow pieces of double sticky tape sandwiched between a cover glass and the microscope slide. All measurements were done  $\sim 5 \mu\text{m}$  from the surface where the influence of the surface on the viscous drag coefficient was smaller than 6%.

### 3. Experimental results

The data shown in Fig. 2 was obtained by a back-and-forth displacement of the trap of 77 nm. This pattern was repeated 100 times, and the averaged data fitted with Eq. (3) using Labview 8.2 or IGOR Pro 5.0 (for off-line analysis). Upon a rapid stepwise displacement of the trap the bead is expected to relax back to the center of the trap according to:

$$X(t) = X_0 e^{-t/t_b} \quad (1)$$

where  $X(t)$  is the time-dependent bead displacement from the center of the trap,  $X_0$  the initial displacement of the trap, and  $t_b = \beta/k$  the typical relaxation time of the bead in the trap with  $\beta$  the viscous drag coefficient for the bead and  $k$  the trap’s spring constant. However, the data recorded and shown in Fig. 2 do not fit this simple equation due to limited time response of the QPD when used at a wavelength of 1064 nm. Berg-Sørensen et al. [9] analyzed the temporal response of the silicon QPD detectors as a function of wavelength. The transparency of silicon at 1064 nm was found to cause a time response delay of the detector due to charge carriers created in the n-layer, where they are transported by thermal diffusion, instead of being created in the depletion area where they are detected at the nanosecond timescale. The QPD temporal response was found to obey:

$$g(t) = \alpha \delta(t) + (1 - \alpha) \frac{1}{t_d} e^{-t/t_d} \quad (2)$$

with  $\alpha$  the fraction of charge carriers created in the depletion area,  $\delta(t)$  the Dirac function describing the instantaneous response and  $t_d$  the time response of the QPD for charge carriers created in the n-layer. The measured bead response upon a stepwise trap displacement is then given by the convolution of  $X(t)$  and  $g(t)$ :

$$S(t) = \int_0^t X(t)g(t-t')dt = X_0 \alpha e^{-t/t_b} + X_0 (1 - \alpha) \frac{t_b}{t_b - t_d} \left( e^{-t/t_b} - e^{-t/t_d} \right) \quad (3)$$

This equation fits the dimensionless data in Fig. 2.  $\alpha$ ,  $t_b$  and  $t_d$  are free parameters. With  $X_0 = 77$  nm the initial and known displacement of the trap, we then obtain the calibration of the position sensor in unit of 1/nm. At the same time the trap spring constant  $k$  is derived from  $t_b$  with knowledge of the viscous drag coefficient of the bead ( $\beta = 6\pi\eta r$ , with  $\eta$  the viscosity and  $r$  the radius of the bead).

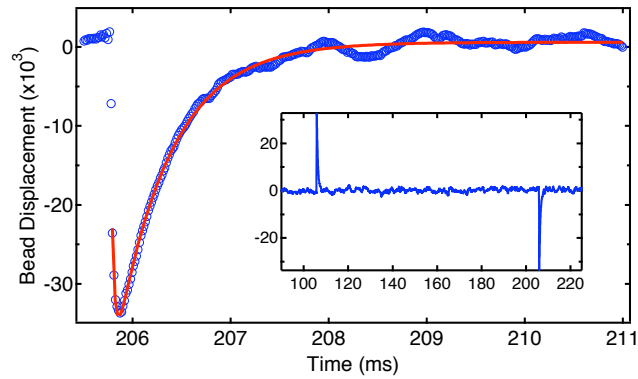


Fig. 2. Computed displacement in dimensionless units of a trapped silica bead of diameter  $1 \mu\text{m}$ . Displacement of  $77 \text{ nm}$  of the trap was repeated 100 times and QPD signal (blue circles) was averaged before being fitted by Eq. (3) (red line). The inset shows the whole acquired signal and the main graph shows a zoom of the second peak fitted with Eq. (3). The averages of the fitting parameters for the two peaks give a detector calibration of  $0.515 \text{ pm}^{-1}$ , a cutoff frequency of the trap of  $302 \text{ Hz}$ , a fraction of instantaneous response of the QPD of  $\alpha = 0.36$ , and a cutoff frequency for the QPD of  $6341 \text{ Hz}$  (indeed 100 times lower than the AOD bandwidth and 10 times lower than the sampling rate).

Figure 3 shows the dimensionless values  $X_0$ , as found from the fits, as a function of trap displacement in units of nanometers, yielding a linear detector response for displacements of up to  $150 \text{ nm}$  from the trap center. Since the position calibration depends upon a fit of the dynamics response of the bead in a harmonic trap potential, the divergence from linear behavior is likely due to non-linearities in the BFP detection method and any non-harmonicity of the trap potential this far out from the trap center.

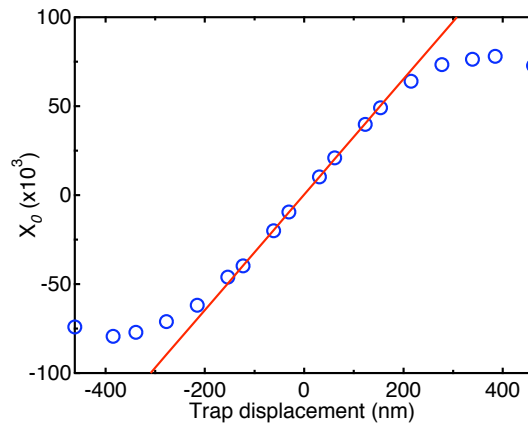


Fig. 3. Linearity of detector response. Blue circles represent the experimental data and the red line the fit of the linear region of the trap. Experimental data show a linear range of the detector response of  $\pm 150 \text{ nm}$  with a slope of  $0.324 \pm 2 \cdot 10^{-3} \text{ nm}^{-1}$  and an intersection with the vertical axis at  $0.3 \pm 0.2$  (dimensionless).

Typical errors in position detector calibration and trap spring constant were estimated

by repeating the method 10 times with a single bead. We found a detector response of  $0.512 \pm 0.013 \mu\text{m}^{-1}$  (mean  $\pm$  s.d.) so with comparable precision as scanning the bead with the laser as reported in [8] and a time response of the bead of  $0.532 \pm 0.027$  ms (i.e. a spring constant of  $0.0188 \pm 0.0010$  pN.nm $^{-1}$ ) which proves the method to be highly reproducible. In addition we recorded the Brownian motion of the same bead at 65536 Hz for 8 seconds. We then compared our method to the power spectral method by Berg-Sørensen et al. [10] which also takes into account the limited temporal response of the QPD using their Matlab utility [11]. The time response of the bead thus found was  $t_b = 1/2\pi f_c = 0.555 \pm 0.013$  ms with  $f_c$  the cutoff frequency of the PSD and a spring constant computed as  $0.0183 \pm 0.0004$  pN.nm $^{-1}$ . Multiplying the PSD with the frequency squared as described by Allersma et al. in [7] also allows one to get the detector response, calculated here as  $0.479 \pm 0.007 \mu\text{m}^{-1}$ . Both values of the spring constant and the detector response are in good agreement with our method. It should also be mentioned that when using a stiff trap the latter method shows some limitations due to the limited time response of silicon detectors while our method remains valid if the sampling rate is high enough.

To test our position detection calibration value of  $0.512 \mu\text{m}^{-1}$ , we used it to convert the particle's displacement,  $x$ , measured as a dimensionless quantity on our QPD, in units of length. We could then compute the spring constant from the equipartition theorem method  $k = k_B T / \langle x^2 \rangle$  with  $k_B$  the Boltzman constant and  $T$  the absolute temperature. We found a spring constant of  $0.0175$  pN.nm $^{-1}$ , consistent with the spring constant derived from  $t_b$  using our method and with the cutoff frequency found using Berg-Sørensen et al. power spectral method [10] as reported above. The somewhat lower value obtained using the equi-partition method is consistent with the notion that the slow drift may accumulate, increasing the variance and thus underestimating  $k$ , whereas our jump method and power spectral method, in practice, prove much less sensitive to such drift.

#### 4. Conclusion

We have demonstrated a new calibration method that has the advantage of inferring both trap and detector calibrations using a single laser and standard acousto-optic deflector. The limited time response of the QPD detector is properly taken into account. As with most other methods, the bead diameter, as well as the temperature and the medium viscosity, have to be known. This calibration can be performed rapidly on the same bead as will then be used for the experiment, and in the same trapping conditions. Through comparison with other existing methods, we have shown that the calibration parameters from this simple method are both precise and accurate.

#### Acknowledgments

We thank Frédéric Moron for technical support on the detection electronics. This work has been supported by the Region Ile-de-France in the framework of C'Nano IdF. C'Nano IdF is the nanoscience competence center of Paris Region, supported by CNRS, CEA, MESR and Region Ile-de-France. KV's stay in Institut d'Optique was financed by grants from Université Paris Sud XI and CNRS.